ELSEVIER

Earth and Planetary Science Letters 139 (1996) 63–78

EPSL

Paleomagnetism of the Lesotho basalt, southern Africa

Andrei A. Kosterov [a,1,b], Mireille Perrin [a,*]

[a] *Laboratoire de Géophysique et Tectonique, URA CNRS 1760, Université Montpellier II Case 060, 34095 Montpellier Cedex 5, France*
[b] *Earth Physics Department, Institute of Physics, Sanct-Petersburg University, Petergoff, Sanct-Petersburg 198904, Russia*

Received 30 June 1995; accepted 28 December 1995

Abstract

Paleomagnetic study of four sections from Middle Jurassic Karoo lava, located in Lesotho and South Africa, yielded a new paleomagnetic pole for Africa with coordinates 71.6°N, 273.5°E ($A_{95} = 3.7°$, $K = 33$, $N = 47$). Paleosecular variation, estimated as the angular standard deviation of VGPs distribution is 14.1° (+2.4°/− 1.8°), which is considerably lower than expected for this time interval and latitudinal band. Preliminary paleointensity results indicate a low field intensity during the acquisition of the magnetization, this new result tends to support a possible correlation between secular variation and dipole intensity. When the lower to middle Jurassic paleomagnetic data set for Africa is considered, a difference of 13.9 ± 8.7° of arc is found to exist between the mean Northwest and South African poles. Furthermore, while the Northwest African pole is in very good agreement with the lower to middle Jurassic North American pole, whichever set of rotation parameters is used to close the North Atlantic ocean, the South African pole falls some 12–15° of arc apart. As intraplate deformation models, developed to achieve tighter fit of West Gondwana prior to the opening of the South Atlantic, fail to account fully for the difference between Northwest and South African poles, the pre-Cretaceous Apparent Polar Wander Path for Africa has to be considered with caution.

Keywords: Karoo Igneous Province; South Africa; Lesotho; paleomagnetism; Middle Jurassic; apparent polar wandering

1. Introduction

Basalts of the Karoo Igneous Province are the most significant manifestation of the Lower Jurassic magmatic activity which preceded the break-up of Gondwana [1,2]. Almost everywhere, the volcanic members rest on sedimentary rocks of the Karoo Supergroup, an intracratonic basinal sequence of Late Carboniferous to Triassic age. The tholeiitic lava flows form, in particular, the huge Lesotho basaltic plateau, which is 300 km wide and reaches 3500 m above sea level. The maximum thickness of the lava pile appears to be > 1500 m [3].

A chemical and magnetic stratigraphy of the low-Ti basalt of Lesotho was proposed [4] with eight magma types and eleven stratigraphic units. A magnetic reversal, going from reverse to normal, is found in the lower quarter of the pile. Over a thickness of some 150 m, intermediate directions are recorded and the detail of the reversal, initially studied by Van Zijl et al. [5], has been revisited [6]. Major and trace element analyses show the basal flows to have consistently higher Zr to P ratios than those above [3].

* Corresponding author. E-mail: perrin@dstu.univ-montp2.fr
[1] Université Montpellier II E-mail: kostero@dstu.univ-montp2.fr; Sanct-Petersburg University E-mail: kosterov@phim.niif.spb.su

PII S0012-821X(96)00005-2

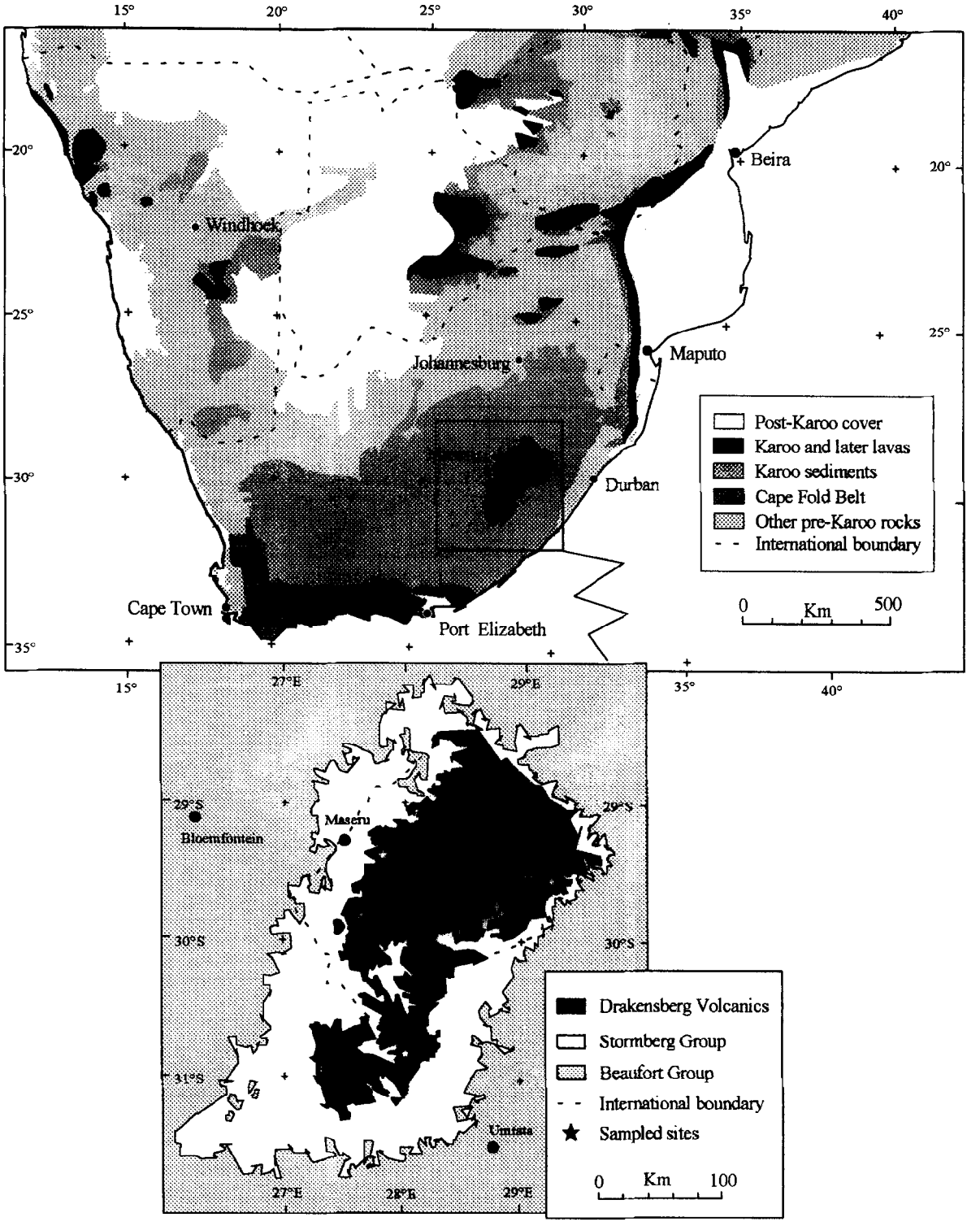
15°
20°
25°
30°
35°
40°
20°
25°
30°
35°
Beira
Windhoek
Maputo
Johannesburg
Durban
Cape Town
Port Elizabeth
Post-Karoo cover
Karoo and later lavas
Karoo sediments
Cape Fold Belt
Other pre-Karoo rocks
International boundary
0 Km 500
27°E
29°E
25°S
29°S
30°S
31°S
Maseru
Bloemfontein
Umtata
Drakensberg Volcanics
Stormberg Group
Beaufort Group
International boundary
Sampled sites
0 Km 100

The lower, thin units, which display diverse composition, are overlain by a main sequence of thick units of less variable composition [7]. Lower units in North and South Lesotho differ, indicating separate eruption sites and a topographic barrier between these two areas during the earliest eruptions. In contrast, the upper units occur with regular thickness throughout the basalt remnant, suggesting uniform eruption onto a planar surface. Dating Karoo igneous rocks by the conventional K–Ar and $^{40}Ar/^{39}Ar$ age spectrum methods lead Fitch and Miller [8] to propose two major magmatic events, at 193 ± 5 and 178 ± 5 Ma, with minor activity around 204 and 186 Ma; the Lesotho lavas being erupted during the first major event. However, recently this chronology was questioned and new $^{40}Ar/^{39}Ar$ dates from top to bottom of the pile fall within 180 ± 2 Ma [3,7], suggesting a short period of magmatic activity.

The quality of the magnetic field recording in the Karoo basalt, shown by previous studies, led us to sample these rocks again in order, this time, to find the intensity of the paleomagnetic field in the Lower Jurassic. Prior to paleointensity determinations, classic paleomagnetic and rock magnetic analyses were carried out. This paper will focus on these results and, in particular, the recording of secular variation and geodynamic implications.

2. Sampling

The goal of this new sampling (412 oriented cores from 77 lava flows) was to find sequences as long as possible in both normal and reverse parts of the section, while staying away from the intermediate zone as long as we were interested by the characteristics of the mean dipole field. The sampling of a large number of flows is crucial in this case because each individual flow acquires its magnetization rapidly while cooling, and therefore represents an instantaneous reading of the magnetic field and, in order to estimate the intensity of the mean dipole field, secular variation has to be averaged out. In the upper normal sequence, an almost complete sequence was available along the newly built road going from Pitseng to Mafika Lisiu Pass (Fig. 1, mean coordinates 29.07°S, 28.38°E) which cut new outcrops with over a hundred flows, easily recognizable and corresponding to a total thickness of the order of a thousand meters. One of every two flows was systematically sampled (47 flows and 248 samples) and relative altitudes of each flow estimated with an altimeter. For the lower reverse interval, unfortunately, such a sampling was impossible and no complete sequence could be found. Therefore we had to sample three different sections hoping to cover as much of the reverse interval as possible. In Lesotho, we sampled one of Van Zijl et al.'s [5] sites near Sani Pass (Fig. 1 and 29.60°S, 29.33°E). There, 23 successive reverse flows could be found before the transitional zone and again one of every two flows was sampled (17 flows and 86 samples). We sampled another site in Lesotho near Nazareth (Fig. 1 and 29.41°S, 27.82°E), located directly at the base of the transitional Bushman section, which was sampled by Prevot et al. [6], to restudy the detail of the magnetic reversal. There, only 5 reverse flows (35 samples) could be found. Finally, a last reverse section was sampled in South Africa, near Rhodes (Fig. 1 and 30.76°S, 28.02°E), with 8 flows and 43 samples. Cores were drilled directly in the field with a portable gasoline-driven drill and oriented using both magnetic and sun compasses. Lava flows being essentially flat-lying throughout the whole plateau, no tilt correction was applied.

3. Experimental techniques

Alternating field (AF) demagnetization and thermal cleaning in air were used to isolate the characteristic remanent magnetizations (ChRM). After each step of the thermal treatment, low field susceptibility was measured at room temperature in order to determine any mineralogical changes. Any variation between thermal and AF cleaning was checked by a direct comparison of results obtained from sister specimens of the same core. The two ways of clean-

Fig. 1. Simplified geological map of Karoo rocks, modified after Eales et al. [1] with insert showing sampling localities, modified after Kitchin and Raatch [51].

ing were shown to yield identical results and will be hereafter considered as equivalent. The determination of ChRM was made by principal component analysis [9]. Magnetic viscosity indices [10,11] were estimated for all samples of the collection by measuring the remanent magnetization, first after 2 weeks of storage with the ambient field parallel to the cylindrical axis of each specimen, and then after another 2 weeks of storage in zero field. The viscosity indices reflect the capacity of the samples to acquire viscous remanent magnetizations (VRM) and are a very useful criteria for selecting reliable samples. All remanences were measured with a 2G cryogenic magnetometer. Susceptibilities were measured with a Bartington susceptibility meter MS-2.

4. Paleodirectional results

4.1. Mafika Lisiu Pass section

Thirty seven samples belonging to 29 lava flows (out of 47 sampled) were subjected to thermal cleaning and 159 samples were AF demagnetized to obtain the ChRM directions. When possible, the cores with minimum viscosity indices were chosen for both thermal and AF treatments. Examples of orthogonal diagrams are given in Fig. 2 for both thermal and AF demagnetization. Most of the samples showed predominantly single component magnetization. Small secondary components, probably laboratory induced, were removed at 50–10 mT or 100–250°C. The quality of the paleomagnetic data is generally very high, mean angular deviations (MAD, [9]) of ChRM being well below 1° and frequently below 0.5°. The almost unique exception is flow 64, which shows evident signs of remagnetization by lightning: a high natural remanent magnetization (NRM) intensity, large and chaotic scatter of NRM directions and instability to AF treatment. However, the ChRM directions still could be retrieved for 3 out of 5 samples from this flow.

According to their magnetic properties, samples clearly form two different groups. The first one, mainly represented by gray-colored samples, is characterized by maximum unblocking temperatures below 600°C. The median destructive field of NRM for these samples is apparently normally distributed, with a rather sharp mode in the range 20–25 mT. These features suggest the presence of almost pure magnetite as the major remanence carrier although, for some samples of this group, thermal demagnetization curves indicate the presence of some minor, more titanium-rich, phase with a Curie point around 400°C. About 80% of the samples belong to this first group. The second group has quite distinctive rock magnetic properties and is represented by reddish to brownish colored samples which have maximum unblocking temperatures above 600°C and NRM median destructive fields in the range 40–60 mT. In this case, even if low-Ti magnetite seems to be the major magnetic mineral, a fraction of the magnetization is carried by

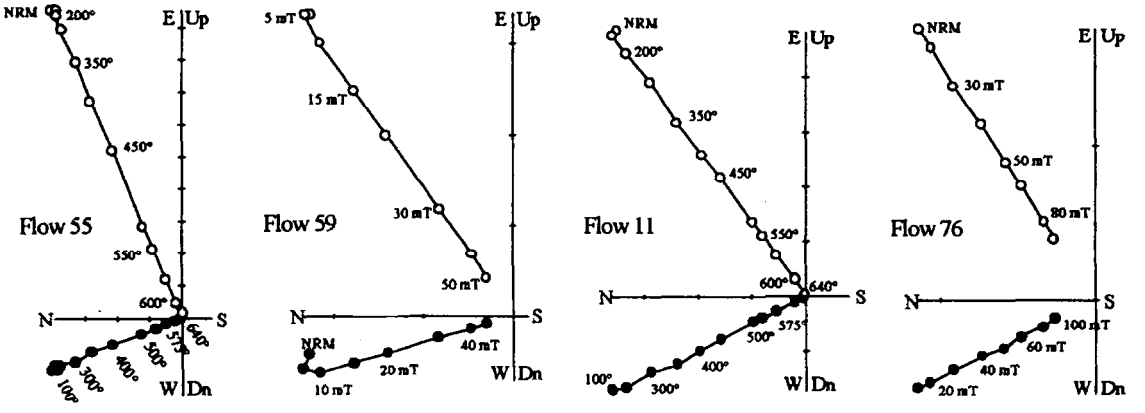

Fig. 2. Examples of orthogonal diagrams from the normal section after thermal and AF demagnetization. ○ = vertical planes; ● = horizontal planes. Units are in $A \cdot m^2/kg$.

hematite.

Flow mean directions were calculated from, at least, three cleaned samples per flow. These mean directions are listed on the left-hand side of Table 1 and the evolution along the section is shown in Fig. 3. It is obvious that some flow mean directions can be further united into directional groups, which are more likely to represent independent spot readings of the Earth's magnetic field. We consider that successive flows belong to the same directional group if: (1) their confidence circles overlap significantly; and (2) there is no evident directional trend between the flows. Twenty eight directional groups were distinguished (right-hand side of Table 1). The lowermost (flows 3–13) and the uppermost parts (flows 71–84 and 88–93) of the section, where several flows have essentially the same directions, may correspond to very rapid eruption episodes, while the middle part of the section seems to have formed in a slower regime.

4.2. Sani Pass section

Among the three reverse sections sampled, the Sani Pass section is the most extensive. Samples from all 17 flows sampled were subjected to either thermal (43 samples) or AF (42 samples) cleaning. Representative orthogonal diagrams are given in Fig. 4. The viscosity indices of these rocks are significantly greater than those of the Mafika samples, and secondary overprints, probably of viscous origin, are more important. Nonetheless, the definition of ChRM was straightforward, apart from some particular cases. However, we sometimes had to reject samples with evident outlier directions. An extreme case is flow 17, for which only 2 out of 5 samples seem to have preserved the original field direction, whereas directions of 3 other samples clearly tend towards the mean direction of the overlying flow 18. Very likely, flow 17 (5 m thick) was partially remagnetized by flow 18, which is three times thicker.

From the point of view of magnetic properties, most of the Sani Pass samples are quite similar to the first group of Mafika samples, although they are generally slightly less resistant to AF demagnetization. Maximum unblocking temperatures are normally in the range 525–575°C and sometimes above 600°C. However, some samples from flows 18 and 20–21A have rather peculiar magnetic properties.

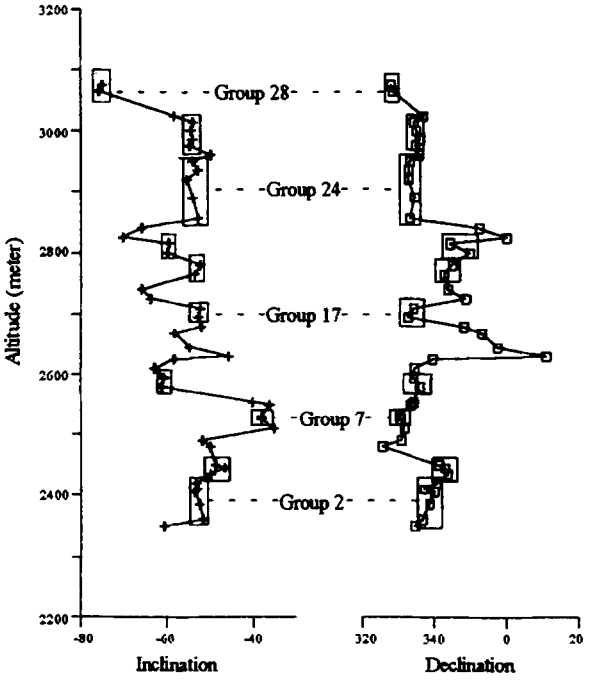

Fig. 3. Evolution of paleomagnetic field direction along the Mafika section. Directional groups are shown by rectangles.

Table 1
Paleomagnetic results for the Mafica section

Flow	Alt, m	n \ N	Inc	Dec	k	a95	Group	Inc	Dec	k	a95	VGP Lat	VGP Long
101	3075	3 \ 3	-74.9	328.1	1738	3.0	28	-75.4	328.3	2665	1.3	50.8	231.0
100	3065	3 \ 3	-75.8	328.5	3680	2.0							
95	3025	4 \ 5	-58.3	337.1	1028	2.9	27	-58.3	337.1	1028	2.9	68.7	264.7
93	3015	3 \ 3	-54.0	334.5	1601	3.1	26	-54.3	335.2	2938	0.8	68.2	276.6
91	3000	3 \ 3	-54.5	335.2	2683	2.4							
89	2985	3 \ 3	-54.1	336.2	2618	2.4							
88	2975	3 \ 3	-54.8	334.9	3641	2.0							
86	2960	5 \ 5	-49.9	336.0	3303	1.3	25	-49.9	336.0	3303	1.3	69.2	287.9
84	2950	3 \ 3	-54.0	333.3	4423	1.9	24	-53.8	333.5	2661	0.7	66.9	278.3
82	2935	3 \ 3	-52.8	333.1	1799	2.9							
80	2920	3 \ 3	-55.4	333.0	8573	1.3							
76	2890	3 \ 3	-54.1	334.8	4587	1.8							
71	2855	3 \ 3	-52.8	333.4	3857	2.0							
69	2840	4 \ 4	-65.9	352.7	805	3.2	23	-65.9	352.7	805	3.2	70.1	222.8
67	2825	5 \ 5	-70.2	0.3	9862	0.8	22	-70.2	0.3	9862	0.8	64.9	207.9
66	2815	3 \ 3	-59.6	344.6	632	4.9	21	-59.7	347.3	647	2.6	74.5	247.1
64	2800	3 \ 5	-59.8	350.0	704	4.6							
61	2780	3 \ 3	-52.4	345.2	1970	2.8	20	-53.0	344.1	2472	1.3	75.7	276.0
59	2765	3 \ 3	-53.6	342.9	8505	1.3							
55	2740	5 \ 5	-65.8	344.0	1933	1.7	19	-65.8	344.0	1933	1.7	67.4	237.0
53	2725	5 \ 5	-63.7	348.9	1433	2.0	18	-63.7	348.9	1433	2.0	71.4	234.6
51	2710	3 \ 3	-52.4	334.4	1318	3.4	17	-52.6	333.6	1436	1.8	67.1	281.3
49	2695	3 \ 3	-52.9	332.8	1188	3.6							
47	2680	5 \ 5	-52.2	348.3	1235	2.2	16	-52.2	348.3	1235	2.2	79.3	275.2
45	2670	5 \ 5	-58.3	353.3	1491	2.0	15	-58.3	353.3	1491	2.0	78.7	235.9
43	2645	9 \ 9	-54.8	357.7	155	4.1	14	-54.8	357.7	155	4.1	83.0	225.3
41	2630	5 \ 5	-45.8	11.1	3322	1.3	13	-45.8	11.1	3322	1.3	80.0	110.2
39	2625	4 \ 5	-58.4	339.6	288	5.4	12	-58.4	339.6	288	5.4	70.4	262.2
37	2610	5 \ 5	-62.9	334.6	432	3.7	11	-62.9	334.6	432	3.7	64.7	254.3
35	2595	5 \ 5	-60.7	334.4	1132	2.3	10	-61.0	335.2	675	1.9	66.2	258.8
33	2580	5 \ 5	-61.2	336.1	424	3.7							
30	2555	5 \ 5	-40.3	334.3	636	3.0	9	-40.3	334.3	636	3.0	66.2	307.3
29	2550	4 \ 5	-36.2	333.5	1229	2.6	8	-36.2	333.5	1229	2.6	64.4	312.8
27	2530	5 \ 5	-38.2	330.4	280	4.6	7	-38.1	330.5	466	2.2	62.3	307.7
26	2525	5 \ 5	-38.0	330.7	807	2.7							
24	2510	5 \ 5	-35.3	331.7	1254	2.2	6	-35.3	331.7	1254	2.2	62.5	312.4
22	2490	5 \ 5	-51.9	330.9	787	2.7	5	-51.9	330.9	787	2.7	64.8	283.2
21	2480	5 \ 5	-50.0	325.6	3899	1.2	4	-50.0	325.6	3899	1.2	60.2	286.5
18	2450	4 \ 4	-48.8	341.4	339	5.0	3	-48.5	342.6	540	2.1	74.9	292.7
17	2445	3 \ 3	-46.7	343.1	478	5.6							
15	2435	3 \ 3	-49.9	343.9	4439	1.9							
13	2420	3 \ 3	-53.3	340.6	514	5.4	2	-52.8	338.7	891	1.3	71.4	279.7
11	2410	3 \ 3	-53.0	337.3	678	4.7							
9	2405	3 \ 3	-53.5	340.2	545	5.3							
7	2385	3 \ 3	-52.4	338.8	11491	1.2							
3	2360	3 \ 3	-51.7	336.9	906	4.1							
1	2350	5 \ 5	-60.7	334.8	2865	1.4	1	-60.7	334.8	2865	1.4	66.0	259.9
Mean							28(186)	-55.1	340.2	49	3.9	72.0	268.2
												K = 38	A_{95} = 4.5

They are generally much more weakly magnetized than 'regular' samples and present two phases with very different coercivities: a 'magnetite-like' phase, the magnetization of which is removed in fields of the order of 50–70 mT, and a 'hematite-like' phase which cannot be effectively demagnetized even in the highest field (200 mT) available in the laboratory. Unfortunately, when heated in air above 500°C, all these samples undergo strong chemical transformation producing new magnetic phases (most probably magnetite), which is indicated by an enormous (sometimes up to ten times) increase in low-field susceptibility measured after heating. This means that it is impossible to verify the presence of an hematite-like phase from thermal demagnetization experiments.

The paleomagnetic directions obtained for the Sani Pass section are listed in Table 2. Here, contrary to the Mafika section, the directional groups include, at the most, two flows. Data quality is also fairly high, although we had to remove some samples which either fail to yield a reliable ChRM direction or give an aberrant direction, which can be caused either because of strong alteration or orientation errors. As mentioned above, flow 17 shows clear evidence of large remagnetization by overlying flow 18 and was therefore rejected.

4.3. Nazareth section

Eleven samples, from flows 1, 3, 4 and 5, were subjected to thermal treatment and 18 samples from all 5 flows to AF cleaning. Several examples of orthogonal diagrams are given in Fig. 4. Flow 2 and, in part, flow 1 appear to be affected by lightning, which is evident from anomalously high NRM intensities and weak resistance to AF treatment. Only a very crude estimation of ChRM directions is possible for 4 out of 5 samples from flow 2. The 'ChRM' directions for this flow are very poorly clustered and were rejected from the analysis. Contrary to flow 2, flow 1 samples appear to be only partially remagnetized by lightning and appropriate AF cleaning succeeded in isolating the characteristic remanence. For flow 4, 2 out of the 6 samples were drilled in the proximity of dynamite holes and probably were remagnetized by shock. These two samples failed to yield reliable ChRM. The 4 remaining samples yielded fairly consistent directions. Flows 3 and 5 yield reasonably clustered ChRM directions (Table 2).

4.4. Rhodes section

Twenty one samples were subjected to thermal and 12 to AF cleaning, representative orthogonal diagrams are given in Fig. 4. Four of the 8 flows which were sampled (flows 4, 5, 7 and 8) yielded directions which, after thermal cleaning, seem to be intermediate. As this study is focused on the behavior of Earth's magnetic field during stable polarity epochs, these 4 flows were not considered further. Results for the remaining 4 flows are given in Table 2. Two of them (flows 1 and 6, the latter being stratigraphically directly above flow 1) reveal identical flow mean directions and were therefore united into a directional group. The overall quality of paleomagnetic data were not as high as for Mafika or Sani Pass sections, with the exception of flow 6, which yielded an excellent paleodirection determination. The 3 others are much poorly clustered, and for both flow 2 and 3, we had to reject one outlier sample.

5. Paleomagnetic pole position

Virtual geomagnetic poles (VGPs) were calculated using the mean directions of the directional groups (Fig. 5a) considered, as already said, to be instantaneous readings of the Earth's magnetic field. As both normal and reverse directions are present, a

Note to Table 1:
Flow and Group = the flow and the directional group numbers in the stratigraphic column; Alt = the flow altitude in meters; n\N = the number of samples used\treated for the determination; Inc, Dec = the inclination and declination of the ChRM; k, a95 = the precision parameter and the confidence cone of the Fisher statistic; and VGP Lat and VGP Long = the latitude and longitude of the Virtual Geomagnetic Pole.

reversal test is possible. The distribution of VGPs for both normal and reverse sections is given in Fig. 5b. For the normally magnetized Mafika section, the paleomagnetic pole coordinates are 72.0°N, 268.2°E (A_{95} = 4.5°, K = 38, N = 28); for the three reverse sections, the mean VGP plots at 70.7°S, 100.8°E (A_{95} = 6.6°, K = 27, N = 19). The angle between the normal pole and the reverse pole is only 4.2°, which is less than each of the A_{95} values. The critical angle, for which these poles would be differ-

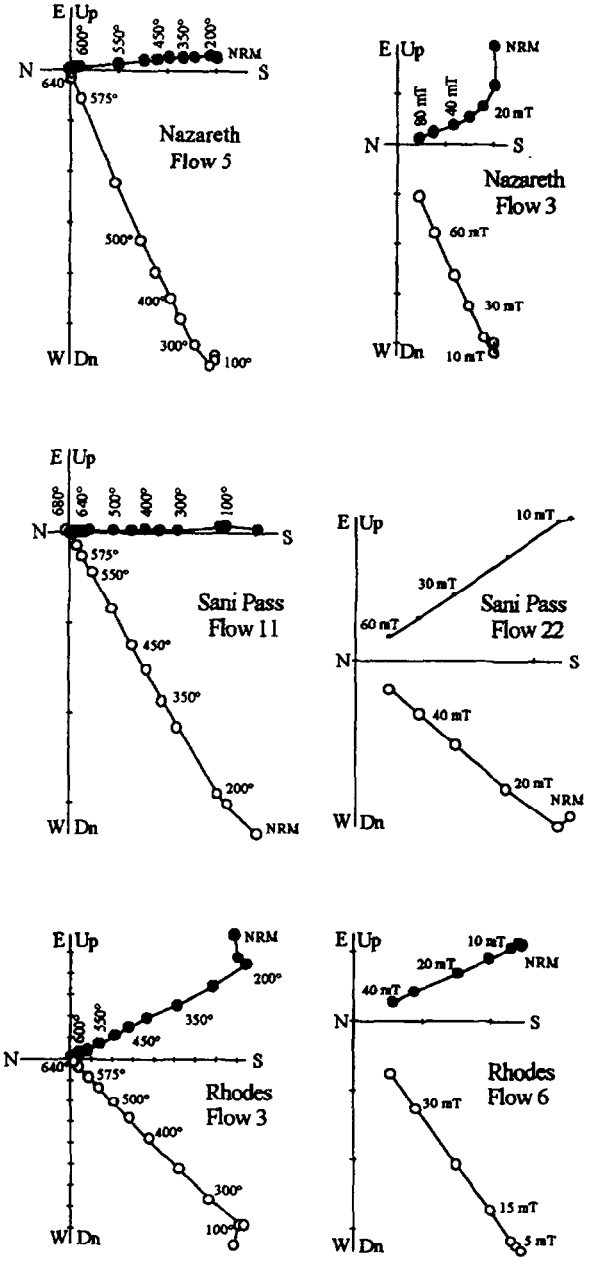

Fig. 4. Examples of orthogonal diagrams from the reverse sections after thermal and AF demagnetizations. ○ = vertical planes; ● = horizontal planes. Units are in A · m^2/kg.

ent at the 95% level, is 7.5°. Thus, the collection passes the reversal test at level B, following the classification of McFadden and McElhinny [12]. Finally, the coordinates of the mean paleomagnetic pole from both normal and reverse sections are 71.6°N, 273.5°E (A_{95} = 3.7°, K = 33, N = 47).

It is worth noting the amazing correlation between this pole and the one published by Van Zijl et al. [5], more than 30 years ago. These two poles are statistically identical, not only does our pole lie within the large (15°) cone of confidence of Van Zijl et al.'s one, but this latter is as well within the much smaller (3.7°) cone of confidence of our pole. Even though we sampled one of Van Zijl et al.'s sections, a

Table 2
Paleomagnetic results for the three reverse sections

Flow #	Alt, m	n\N	Inc	Dec	k	a95	Group #	Inc	Dec	k	a95	VGP Lat	VGP Long
Sani Pass													
22	2390	5\5	36.8	146.1	1188	2.2	12	36.8	146.1	1188	2.2	-58.1	127.9
21a	2340	3\6	40.8	152.2	460	5.8	11	38.6	152.1	394	2.8	-63.7	130.2
21	2335	5\5	37.3	152.0	404	3.8							
20	2330	4\5	41.1	146.2	497	4.1	10	40.6	146.4	376	2.9	-59.3	123.3
19	2300	4\5	40.1	146.6	245	5.9							
18	2285	4\5	41.0	140.0	9311	1.0	9	41.0	140.0	9311	1.0	-53.9	119.4
17	*2270*	*2\5*	*60.1*	*160.0*	-	-							
16	2265	4\4	40.4	159.7	247	5.9	8	40.4	159.7	247	5.9	-70.7	134.5
15	2255	4\5	39.7	154.2	1923	2.1	7	39.7	154.2	1923	2.1	-65.9	130.3
14	2240	4\5	54.7	164.3	2575	1.8	6	54.7	164.3	2575	1.8	-75.6	92.4
13	2235	4\5	69.5	187.1	1024	2.9	5	69.5	187.1	1024	2.9	-65.8	18.8
11	2230	5\5	61.8	177.8	1044	2.4	4	61.8	177.8	1044	2.4	-76.5	36.2
10	2210	3\5	55.0	179.9	1652	3.0	3	53.9	177.6	977	1.8	-84.7	51.9
8	2170	5\5	53.2	176.2	1100	2.3							
4	2125	4\4	59.7	154.2	1199	2.7	2	59.5	152.9	1233	1.7	-65.4	86.0
2	2100	3\3	59.3	151.1	1195	3.6							
1	2095	5\5	45.9	152.1	457	3.6	1	45.9	152.1	457	3.6	-65.4	117.9
Nazareth													
1		5\5	55.4	148.2	906	2.5	1	55.4	148.2	906	2.5	-62.6	95.7
2		*4\5*	*48.6*	*183.1*	*38*	*15.0*							
3		5\6	60.3	167.5	255	4.8	2	60.3	167.5	255	4.8	-74.5	65.1
4		4\6	72.0	166.5	1613	2.3	3	72.0	166.5	1613	2.3	-60.9	43.1
5		6\6	68.3	171.4	859	2.3	4	68.3	171.4	859	2.3	-67.0	41.6
Rhodes													
1		6\6	51.0	154.8	450	3.2	1	51.2	155.2	779	1.6	-68.9	108.7
6		6\6	51.4	155.7	1788	1.6							
2		4\5	44.0	159.5	360	4.8	2	44.0	159.5	360	4.8	-71.3	128.4
3		4\5	37.9	145.2	157	7.4	3	37.9	145.2	157	7.4	-57.5	126.5
Mean							19 (106)	51.7	156.7	35	5.8	-70.7	100.9
												K = 27	A_{95} = 6.6

Legend as in Table 1. Flow means in italics were not used for group calculation (see text).

precise correlation between the old and the new sampling was not possible and therefore all data could not be combined without taking the chance of bias the main result with non-independent points. The new paleomagnetic study being, however, more detailed than the original study, in both the sampling and the demagnetization techniques and analysis, the later pole position will be considered for the rest of the analysis.

6. Paleosecular variation record

The recording of paleosecular variation (PSV) in lava is a tool for evaluating the quality of a paleomagnetic pole. The axial geocentric dipole takes no account of secular variation, although its effect must be averaged out before paleomagnetic measurements are said to conform with the model. On the other hand, PSV carries information about the behavior of the geomagnetic field during lava eruption and, therefore, the activity of the geodynamo. The secular variation in the past is usually expressed by the scatter in directions obtained in the paleomagnetic study, usually expressed in terms of the angular dispersion estimated from the distribution of the individual directions, assumed to be Fisherian [13]. When dealing with records from different sites, the difference in geographic coordinates of the sampling localities does not allow study of the directions and Virtual Geomagnetic Poles (VGPs) have to be used. The angular standard deviation (a.s.d.) is then estimated from the distribution of VGPs, again assumed to be Fisherian. It was worth noting that these two approaches are somewhat contradictory, because a Fisherian distribution of directions is transformed by the geocentric dipole formula into a non-Fisherian distribution of poles and vice versa [13].

One of the major risk of this analysis, especially when dealing with older rocks, is that only part of the secular variation record will be retrieved, which will cause an artificial underestimation of the secular variation. It is, therefore, very important to test the goodness-of-fit of the Fisher model [14]. Visual examination of the equal-area projection of Mafika directions (Fig. 5a) shows that their distribution is not really Fisherian: no azimuthal uniformity is observed and declinations tend to cluster in two opposite sectors, when considered with respect to the mean direction. This conclusion is confirmed by an uniform quantile–quantile (Q–Q) longitude plot (Fig. 6b). Further, an exponential Q–Q co-latitude plot (Fig. 6a) shows that the entire population is not Fisherian: there is strong lack of directions with co-latitudes between 10–17°, with respect to the mean, as well as some excess of directions with co-latitudes around 20°. The three reverse sections, when combined, also demonstrate an absence of

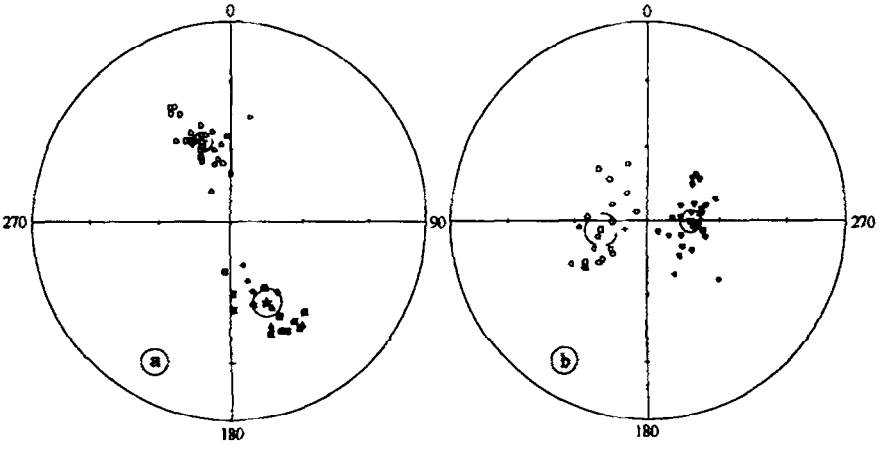

Fig. 5. Equal area projection of (a) paleomagnetic directions and (b) VGPs for all sections. Filled symbols = northern hemisphere; open symbols = southern hemisphere. (a) Circles = the Mafica section; squares = the Sani Pass section; diamonds = the Nazareth section; triangles = the Rhodes section.

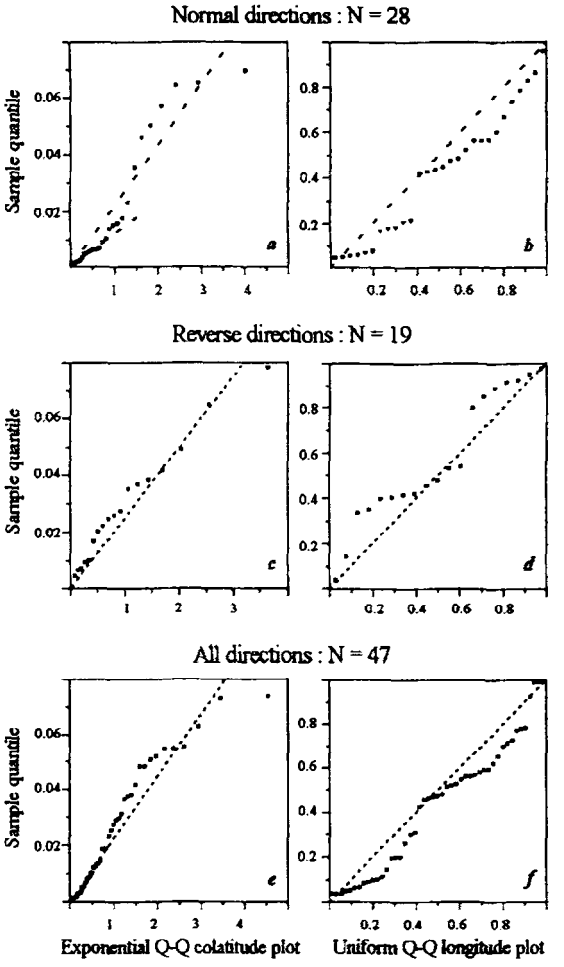

Fig. 6. Probability plots for checking goodness-of-fit of the Fisher distribution to the Karoo paleomagnetic directions. Dotted lines = Fisherian distribution in the exponential Q–Q co-latitude plots and azimuthal uniformity in the uniform Q–Q longitude plots.

azimuthal uniformity (see equal-area projections in Fig. 5a and Q–Q longitude plot in Fig. 6d) and their co-latitudes only very roughly follow Fisher distribution (Fig. 6c). When we turn to the statistical properties of the Mafika VGPs, their longitudes seem to present the same, although less pronounced, type of non-uniformity as that noticed for directions (see uniform Q–Q longitude plot for VGPs in Fig. 7b). However, the exponential Q–Q co-latitude plot (Fig. 7a) shows that co-latitudes of most VGPs, especially with smallest angular deviations from mean, follow more or less a Fisher distribution. The slope of the fitted line, equal to 0.028, yields an estimate of 35.5 for the Fisher precision parameter, which is in reasonable agreement (within 10%) with the calculated value of 38. VGPs of the three reverse sections, when combined, yield a more or less linear Q–Q co-latitude plot (Fig. 7c) with a slope of 0.034, which gives an estimate of 29 for the Fisher precision parameter, in a good agreement with the calculated value of 27. The longitudes of the reverse VGPs (Fig. 7d) tend to cluster into two opposite sectors in the same manner that normal VGPs do. Thus, a lack of azimuthal uniformity shows that the reverse data are also not satisfactorily described by the Fisher distribution. When the entire population of

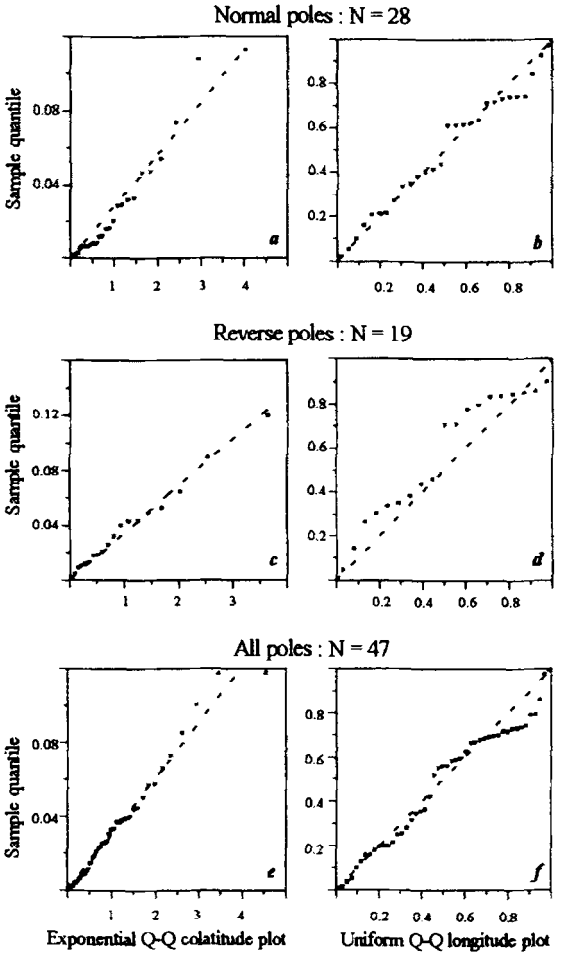

Fig. 7. Probability plots for checking goodness-of-fit of the Fisher distribution to the Karoo paleomagnetic poles. Dotted lines = Fisherian distribution in the exponential Q–Q co-latitude plots and to azimuthal uniformity in the uniform Q–Q longitude plots.

VGPs (normal plus reverse poles) is considered, the Q–Q co-latitude plot (Fig. 7e) appears to be linear for most VGPs, with only the four last points clearly lying apart from the fitted line. The slope of the fit (0.030) yields an estimate of 33 for the Fisher precision parameter, which is equal to the calculated value. Although a certain degree of azimuthal non-uniformity still persists in the entire population of VGPs (Q–Q longitude plot in Fig. 7f), their distribution is reasonably Fisherian and VGPs were used to estimate the a.s.d., which characterizes the paleosecular variation recorded in these lavas.

For all combined VGPs, a.s.d is equal to 14.1° $+2.4/-1.8°$ (95% confidence limit [15]). When compared to the most up-to-date compilation of PSV records in lava [16], this value is significantly lower than the one expected for this latitude (35°) and age interval (110–195 Ma) and is much closer to values for the same latitude band but for younger age intervals (22.5–45 and 45–80 Ma). Preliminary paleointensity results on these Lesotho basalts gave values much smaller than those of the actual field, in agreement with the proposed period of the Mesozoic low field (Mesozoic Dipole Low, [17,18]). Recently, a correlation, based on the analysis of the paleointensity database, was suggested between intensity of the dipole and secular variation [19]. This new result seems to support this idea; however, more studies are needed to reject the alternative hypothesis of data bias in older rocks by insufficient averaging of secular variation before it can be used to constrain geodynamo models.

7. Comparison with previous data and implication for intraplate deformations in Africa

Lower to Middle Jurassic poles published for Africa [20–34] were compiled. Two poles from South Africa [24,25] were rejected because they were not fully based on demagnetization techniques, two other poles from South Africa [20,26], as well as two poles from Northwest Africa [33,34] were also rejected because of the insufficient number of sites and/or samples. Selected poles are listed in Table 3 and plotted in Fig. 8. The most striking feature of this

Table 3
List of Lower to Middle Jurassic African poles

Pole	Rock unit, location	Age in Ma	VGP				Ref
			Lat °N	Long °E	K	A95	
1	Stormberg Lavas, Lesotho	180 ± 5 [7]	72	273	33	4	this study
2	Marangudzi Complex, Zimbabwe	186 ± 3 [35]	70	285	40	9	[21]
3	Mateke Hills Complex, Zimbabwe	177 ± 4	59	260	66	8	[22]
4	Sabie River basalts	178 ± 5 [8]	66	279	24	8	[23]
SA	Southern Africa mean	Jl-Jm	67	273	121	8.4	
5	Hodh, S.Mauritania	187 ± 5	71	240	47	6	[27]
6	Hank, N.Mauritania	187 ± 5	69	232	99	4	[27]
7	Diabase dikes, Liberia	173 - 192	69	242	25	4	[28]
8	Draa Valley sills, Morocco	180 - 186	65	230	121	3	[29]
9	La Reculée, Algeria	180 - 210	71	235	478	2	[30]
10	Illizi basin, Algeria	170 - 190	71	236	334	2	[31, 32]
NWA	North-Western Africa Mean	Jl-Jm	69	236	822	2.3	

Lat and Long = the latitude and longitude of the paleomagnetic poles, respectively; K and A95 = the precision parameter and the 95% confidence cone of the Fisher statistic, respectively. Ages from [7,8,35] where stated.

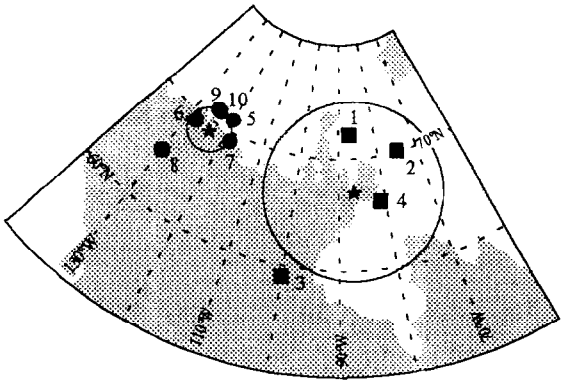

Fig. 8. Equivalent azimutal polar projection of selected lower to middle Jurassic paleopoles for stable Africa (Table 3). ● = northwest Africa; ■ = southern Africa; Stars = the mean Jl–Jm paleopoles with their 95% confidence circles.

data set is that all South African poles lie apart from the poles of Northwest Africa, the angular distance between the two means being 13.9 ± 8.7° of arc.

The first hypothesis to explain this observation would be to consider that the ages are different between the two groups of poles; therefore the gap would reflect the Apparent Polar Wander (APW). However, even if the quality of the age assignments (Table 3) is very variable for the different studies, there is no evidence for a significant age difference between South and Northwest Africa. All Northwest African poles range from 173 to 202 Ma in age, with a mean around 186 Ma, while the South African poles range from 173 to 189 Ma, with a mean around 180 Ma. If this difference was supposed to be significant, that would imply a fairly high APW velocity of the order of 2.5°/Ma.

Other evidence that the position of the South African pole is somewhat anomalous can be obtained from the comparison of the two proposed African poles with the mean Lower to Middle Jurassic (185 Ma) North American pole [36]. Several sets of rotation parameters [37–42] were considered to close the North Atlantic Ocean, and the corresponding positions of the Northwest and South African mean poles are listed in Table 4 in North American coordinates. The Northwest African pole, when rotated to North American coordinates, falls fairly close to the North American one: the angular distance between the two poles ranging from 0.3 to 3°, depending on the continental reconstruction used. In contrast, the South African pole, after rotation to North American coordinates, lies some 12–15° apart from the North American pole. This angle, being of the same order as the one between the two African poles, reinforces the reality of the discrepancy between Northwest and South African pole positions for the Lower to Middle Jurassic.

This means that the rigid plate assumption for Africa, which is anyway only a first-order approximation, has to be rejected. In more recent models of the opening of the South Atlantic Ocean, intraplate deformations in Africa and/or South America are

Table 4
Comparison of the African poles with the mean Lower to Middle Jurassic North American pole proposed by Van der Voo [36] (67°N, 93°E, A_{95} = 4.3°)

Rotation model	Rotation parameters, Afr → NAm			Jl/Jm South African pole rotated to North America			Jl/Jm NW African pole rotated to North America		
	Lat. °N	Long. °E	Angle °	Lat. °N	Long. °E	Gamma °	Lat. °N	Long. °E	Gamma °
Bullard et al. [37]	67.6	346.0	-74.8	81.5	98.0	14.6 ± 9.4	67.7	90.7	1.1 ± 4.3
Le Pichon & Fox [38]	58.3	359.0	-45.3						
	79.1	344.3	-30.4	79.8	91.8	12.8 ± 9.4	65.8	89.1	2.0 ± 4.3
Le Pichon et al. [39]	66.2	347.6	-71.8	81.2	97.9	14.3 ± 9.4	67.3	92.9	0.3 ± 4.3
Lefort [40]	66.0	346.6	-76.7	79.5	87.3	12.6 ± 9.4	65.6	86.3	3.0 ± 4.3
Olivet et al. [41]	66.2	347.3	-76.6	79.5	89.8	12.5 ± 9.4	65.6	87.3	2.7 ± 4.3
Savostin et al. [42]	66.3	342.9	-74.1	82.1	84.6	15.2 ± 9.4	68.2	86.4	2.8 ± 4.3

Gamma is the angle between the SA (NWA) mean pole (Table 3) and North American pole; error is calculated from associated A_{95} values.

assumed to occur in the Lower Cretaceous. Two possible scenario were proposed: the first one, suggested originally by Burke and Dewey [43] and quantified by Pindell and Dewey [44] and Rowley and Pindell [45], implies rather large intraplate deformation within Africa and no deformation within South America. The second one, proposed by Nürnberg and Müller [46], suggests small-scale (normally within 100 km) deformations in narrow zones within both Africa and South America. When the rotation proposed by Rowley and Pindell [45] is applied to the Lower–Middle Jurassic pole for South Africa, it remains some $11.8 \pm 8.7°$ away from the Northwest pole. With the Nürnberg and Müller [46] parameters the angle between the two poles ($14.6 \pm 8.7°$) is larger than without rotation of South Africa. Therefore, these lower Cretaceous intraplate deformations cannot account for the difference in pole positions and some other intraplate deformation seems to have occurred in Africa either before or after the initial opening of the South Atlantic Ocean. There is virtually no paleomagnetic or geological evidence for the first hypothesis, whilst the second seems rather plausible from a geological point of view (see [47,48] and references therein), albeit the chronology of deformations is again uncertain, the ceasing of deformation being rather tentatively placed around 80 Ma. More studies are needed to propose rotation parameters which will fully account for the intraplate deformation in Africa.

The use of pre-Cretaceous South African poles in the calculation of the African APW path, without proper rotation parameters, will therefore introduce errors. To estimate the overall effect, we have recalculated Besse and Courtillot's [49] APWP, but excluding the South African poles. As the Lower to Middle Jurassic (200–170 Ma) APWP segment is well defined from concordant North American and Northwest African data, the removal of the far less numerous South African poles results only in an APWP shift of the order of 1–3°. The effect is bigger for the not so well defined Middle/Upper Jurassic (160–140 Ma) APWP segment, for which the removal of the sole Karoo dolerites pole results in a much greater shift, between 6–9°, although this value is still comparable with the confidence cones of the mean poles. New results, which should be published soon [7,50], will increase the South African data set and help refine the APWP and intraplate deformation models. In the meantime, it is suggested that the South African data should not be used for APW calculation as long as the intraplate deformation is not fully understood.

Acknowledgements

This work was supported by the CNRS–INSU under the DBT program 'Terre Profonde' (Contribution CNRS–INSU–DBT no. 30). A. Kosterov's stay in Montpellier was possible through a grant from the French Government. We thank Michel Prévot (Université Montpellier II), Julian March (Rhodes University, South Africa) and Peter Hooper (Washington State University at Pullman, USA) for their help in the field work. Valuable comments from Michel Prévot, Rob Hargraves, Mike McElhinny and an anonymous reviewer were particularly helpful. *[UC]*

References

[1] H.V. Eales, J.S. Marsh and K.G. Cox, The Karoo igneous province: an introduction, In: Petrogenesis of the Volcanic Rocks of the Karoo Province, A.J. Erlank, ed., Spec. Publ. Geol. Soc. S. Afr. 13, 1–26, 1984.

[2] K.G. Cox, The Karoo province, in: Continental Flood Basalts, J.D. Macdougall, ed., pp. 239–271, Kluwer, Dordrecht, The Netherlands, 1988.

[3] P.R. Hooper, J. Rehacek, R.A. Duncan, J.S. March and A.R. Duncan, The basalts of Lesotho, Karoo Province, Southern Africa, AGU Fall Meeting Trans., p. 553, 1993.

[4] J. Rehacek, P.R. Hooper, R.A. Duncan and J.S. Marsh, Chemical and magnetic stratigraphy of the basalt of Lesotho, Karoo Province, SA, Meeting, A294, 1994.

[5] J.S. Van Zijl, K.W.T. Graham and A.L. Hales, The paleomagnetism of the Stormberg Lavas of South Africa, I. Evidence for a genuine reversal of the Earth's field in Triassic–Jurassic times, Geophys. J. R. Astron. Soc. 7, 23–39, 1962.

[6] M. Prévot, L. Faynot and M. Perrin, Revisiting the Early Jurassic reversal recorded in the Lesotho basalt (Southern Africa), EOS Trans. AGU, 1995.

[7] J.S. Marsh, P.R. Hooper, R.A. Duncan and A.R. Duncan, Stratigraphy and Correlations Amongst Karoo Basalts: Implications for Evolution of the Karoo Igneous Province, IUGG XXI General Assembly, A460, 1995.

[8] F.J. Fitch and J.A. Miller, Dating Karoo igneous rocks by the conventional K–Ar and $^{40}Ar/^{39}Ar$ age spectrum methods, in: Petrogenesis of the Volcanic Rocks of the Karoo Province, A.J. Erlank, ed., Spec. Publ. Geol. Soc. S. Afr. 13, 247–266, 1984.

[9] J.L. Kirschvink, The least squares line and plane and the analysis of paleomagnetic data, Geophys. J. R. Astron. Soc. 62, 699–718, 1980.
[10] E. Thellier and O. Thellier, Recherches géomagnétiques sur des coulées volcaniques d'Auvergne, Ann. Geophys. 1, 37–52, 1944.
[11] M. Prévot, Some aspects of magnetic viscosity in subaerial and submarine volcanic rocks, Geophys. J. R. Astron. Soc. 66, 169–192, 1981.
[12] P.L. McFadden and M.W. McElhinny, Classification of the reversals test in paleomagnetism, Geophys. J. Int. 103, 725–729, 1990.
[13] A. Cox, Latitude dependence of the angular dispersion of the geomagnetic field, Geophys. J. R. Astron. Soc. 20, 253–269, 1970.
[14] N.I. Fisher, T. Lewis and B.J.J. Embleton, Statistical Analysis of Spherical Data, 329 pp., Cambridge University Press, Cambridge, 1987.
[15] A. Cox, Confidence limits for the precision parameter k, Geophys. J. R. Astron. Soc. 17, 545–549, 1969.
[16] P.L. McFadden, R.T. Merrill, M.W. McElhinny and S. Lee, Reversals of the Earth's magnetic field and temporal variations of the dynamo families, J. Geophys. Res. B 96, 3923–3933, 1991.
[17] M. Prévot, M.M. Derder, M. McWilliams and J. Thompson, Intensity of the Earth's magnetic field: Evidence for a Mesozoic dipole low, Earth Planet. Sci. Lett. 97, 129–139, 1990.
[18] M. Prévot and M. Perrin, Intensity of the Earth's magnetic field since Precambrian from Thellier-type paleointensity data and inferences on the thermal history of the core, Geophys. J. Int. 108, 613–620, 1992.
[19] M. Perrin and V.P. Shcherbakov, Phanerozoic paleointensities obtained from volcanic rocks and the reliability of the determinations, IUGG XXI General Assembly, Boulder, USA, B116, 1995.
[20] D.I. Gough and A. Brock, The Paleomagnetism of the Shawa Ijolite, J. Geophys. Res. 69, 2489–2493, 1964.
[21] A. Brock, The paleomagnetism of the Nuanetsi igneous province and its bearing upon the sequence of Karroo igneous activity in southern Africa, J. Geophys. Res. 73, 1389–1397, 1968.
[22] D.I. Gough, A. Brock, D.L. Jones and N.D. Opdyke, The paleomagnetism of the ring complexes at Marangudzi and the Mateke Hills, J. Geophys. Res. 69, 2499–2507, 1964.
[23] D.I. Henthorn, The magnetostratigraphy of the Lebombo group along the Olifants river, Cruger National Park, Ann. Geol. Surv. S. Afr. 15 (2), 1–10, 1981.
[24] M.W. McElhinny and D.L. Jones, Paleomagnetic measurements on some Karroo dolerites from Rhodesia, Nature 206, 921–922, 1965.
[25] M.W. McElhinny, J.S. Briden, D.L. Jones and A. Brock, Geological and geophysical implications of paleomagnetic results from Africa, Rev. Geophys. Space Phys. 6, 201–238, 1968.
[26] A. Gidskehaug, K.M. Creer and J.G. Mitchell, Palaeomagnetism and K–Ar ages of the South-west African basalts and their bearing on the time of initial rifting of the South Atlantic Ocean, Geophys. J. R. Astron. Soc. 42, 1–20, 1975.
[27] B. Sichler, J.L. Oliver, J.M. Auzende, H. Jonquet, J. Bonin and A. Bonifay, Mobility of Morocco, Can. J. Earth Sci. 17, 1546–1558, 1980.
[28] G.B. Dalrymple, C.S. Grommé and R.W. White, Potassium–Argon age and paleomagnetism of diabase dikes in Liberia: initiation of Central Atlantic rifting, Geol. Soc. Am. Bull. 86, 399–411, 1975.
[29] E.A. Hailwood and J.G. Mitchell, Paleomagnetic and radiometric dating results from Jurassic intrusions in southern Morocco, Geophys. J. R. Astron. Soc. 24, 351–364, 1971.
[30] B. Kies, B. Henry, N. Merabet, M.M. Derder and L. Daly, A new Late Triassic–Liassic palaeomagnetic pole from superimposed and juxtaposed magnetizations in the Saharan craton, Geophys. J. Int. 120, 433–444, 1995.
[31] M.M. Derder, B. Henry and N. Merabet, The paleomagnetic results of the Palaeozoic–Mesozoic formations from the Illizi basin (Algeria), Ann. Geophys. Suppl. I–V, 13, 75, 1995 (abstract).
[32] M.M. Derder, personal communication, 1995.
[33] J.C. Briden, D.I. Henthorn and D.C. Rex, Paleomagnetic and radiometric evidence for the age of Freetown igneous complex, Sierra Leone, Earth Planet. Sci. Lett. 12, 385–391, 1971.
[34] C. Bardon, A. Bossert, R. Hamzeh and M. Westphal, Etude paléomagnétique de formations du Trias et du Jurassique du Maroc et du Sahara, C. R. Acad. Sci. Paris Ser. D 276, 2357–2360, 1973.
[35] K.A. Foland and C.M.B. Henderson, Application of age and Sr isotopic data to the petrogenesis of the Marangudzi ring complex, Rhodesia, Earth Planet. Sci. Lett. 29, 291–301, 1976.
[36] R. Van der Voo, Phanerozoic paleomagnetic poles from Europe and North America and comparisons with continental reconstructions, Rev. Geophys. 28, 167–206, 1990.
[37] E.C. Bullard, J.E. Everett and A.G. Smith, A symposium on continental drift. IV: The fit of the continents around the Atlantic, Philos. Trans. R. Soc. London 258, 41–51, 1965.
[38] X. Le Pichon and P.J. Fox, Marginal offsets, fracture zones and the early opening of the North Atlantic, J. Geophys. Res. 76, 6294–6308, 1971.
[39] X. Le Pichon, J.C. Sibuet and J. Francheteau, The fit of the continents around the North Atlantic Ocean, Tectonophysics 38, 169–209, 1977.
[40] J.P. Lefort, Un "fit" structural de l'Atlantique Nord: argumentes géologiques pour correler les marqueres géophysiques reconnus sur les marges, Mar. Geol. 37, 355–369, 1980.
[41] J.L. Olivet, J. Bonnin, P. Beuzart and J.M. Auzende, Cinématique de l'Atlantique Nord et Central, Cent. Natl. Explor. Oceans, Rapp. Sci. Tech. Fr. 54, 108 pp., 1984.
[42] L.A. Savostin, J.C. Sibuet, L.P. Zonenshain, X. Le Pichon and M.J. Roulet, Kinematic evolution of the Tethys Belt from the Atlantic Ocean to the Pamirs since the Triassic, Tectonophysics 123, 1–35, 1986.

[43] K. Burke and J.F. Dewey, Two plates in Africa during the Cretaceous?, Nature 249, 313–316, 1973.

[44] J.L. Pindell and J.F. Dewey, Permo–Triassic reconstruction of Western Pangea and the evolution of the Gulf of Mexico/Caribbean domain, Tectonics 1, 179–211, 1982.

[45] D.B. Rowley and J.L. Pindell, End Paleozoic–Early Mesozoic Western Pangean reconstruction and its implications for the distribution of Precambrian and Paleozoic rocks around Meso-America, Precambrian Res. 42, 411–444, 1989.

[46] D. Nürnberg and R.D. Müller, The tectonic evolution of the South Atlantic from Late Jurassic to present, Tectonophysics 191, 27–53, 1991.

[47] J.D. Fairhead, Mesozoic and Cenozoic plate tectonic reconstructions of the central South Atlantic Ocean: the role of the West and Central African Rift System, Tectonophysics 155, 181–191, 1988.

[48] P. Unternehr, D. Curie, J.L. Olivet, J. Goslin and P. Beuzart, South Atlantic fits and intraplate boundaries in Africa and South America, Tectonophysics 155, 169–179, 1988.

[49] J. Besse and V. Courtillot, Revised and synthetic apparent polar wander paths of the African, Eurasian, North American, and Indian plates, and true polar wander since 200 Ma, J. Geophys. Res. B 96, 4029–4050, 1991.

[50] R.B. Hargraves, Tectonic and geomagnetic significance of Jurassic–Cretaceous paleomagnetic data from Africa, 22nd Earth Science Congr., Geol. Soc. S. Afr., pp. 231–234, 1988.

[51] J.W. Kitching and M.A. Raath, Fossils from the Elliot and Clarens formations (Karoo sequence) of the northeastern Cape, Orange Free State and Lesotho, and a suggested biozonation based on tetrapods, Palaeontol. Af. 25, 111–125, 1984.